

POS0009

The Strain Distribution around Pin-track hole on Varus Femur of The Elderly under Dynamic Loading Conditions

Kittipong Sangrit¹, Kitti Aroonjarattham^{2,*}, Promtpong Anuchitchanchai², Chompunut Somtua^{1,3} and Panya Aroonjarattham¹

¹ Department of Mechanical Engineering, Faculty of Engineering, Mahidol University, Nakornpathom, Thailand, 73170

² Department of Orthopaedics, Faculty of Medicine, Burapha University, Chonburi, Thailand, 20131

³ Department of Mechanical Engineering, Faculty of Engineering, Bangkok Thonburi University, Bangkok, Thailand, 10170

* Corresponding Author: kittaroon@gmail.com

Tel: 66-3839-4850

Abstract

The pin-track hole after total knee arthroplasty was reported the cause of distal femur fracture on post-operative. This hole was used to mark in the computer-assisted navigation surgery process, which was increase the precision of total knee replacement. This research aims to evaluate the maximum equivalent of total strain at pin-track hole on varus femur of the elderly under dynamic walking and dynamic stair-climbing condition. The result of dynamic loading had the higher strain distribution on the pin-track hole than the static loading and the reduction of time cycle, which was represent the accident on the patient had the higher strain distribution on the pin-track hole than the normal time cycle but the dynamic loading did not affect the bone fracture at pin-track hole because all models had the maximum equivalent of total strain on pin-track hole less than 25,000 microstrain.

Keywords: Varus Femur, Dynamic Loading, The Elderly and Pin-track Hole.

1. Introduction

Total knee arthroplasty (TKA) was a surgical process to treat the osteoarthritis that was removed the damaged parts of the knee joint and was replaced with the total knee prosthesis. Computer-assisted navigation in total knee arthroplasty was popularly technique to increase the accuracy for implantation the prosthesis but it had reported the cause of distal femur fracture on post-operative near the pin-track hole region [1]. From previous study [2, 3], the static loading condition did not affect the strain concentration at pin-track hole region that made the distal femur fracture. Therefore, this research aims to use the dynamic loading condition of walking and stair-climbing to analyze the maximum equivalent of total strain at pin-track hole region on varus femur of the elderly by finite element method.

2. Material and Methods

2.1 Three-dimensional models

Three-dimensional model in this research was scanned by computerized tomographic (CT) scanner and reconstruct with ITK-SNAP software. The varus femur bone model was set the position after inserted the femoral component as a neutral alignment and 3 degree valgus alignment [4] as shown in Fig. 1.

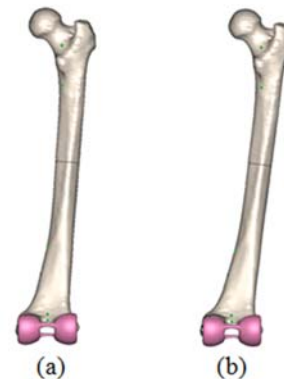


Fig. 1 The position of varus bone model inserted femoral component: (a) Neutral alignment and (b) 3 degree valgus alignment

2.2 Materials Properties

All models were assumed to be linear elastic, homogeneous and isotropic material [4-7]. Material properties of cancellous bone and cobalt-chrome alloy (femoral component) were shown in Table. 1. The material properties of cortical bone of the elderly at 60-89 years for men and women were shown in Table. 2 and 3 respectively.

Table. 1 Materials properties [8, 9].

Materials	Elastic Modulus (MPa)	Poisson's ratio
Cancellous bone	600	0.20
Cobalt-Chrome alloy	230,000	0.30

POS0009

Table. 2 Materials properties of cortical bone for men [10].

Age (years)	Elastic Modulus (MPa)	Poisson's ratio
60-69	15,100	0.30
70-79	14,500	0.30
80-89	12,600	0.30

Table. 3 Materials properties of cortical bone for women [10].

Age (years)	Elastic Modulus (MPa)	Poisson's ratio
60-69	10,800	0.30
70-79	17,600	0.30
80-89	12,600	0.30

2.3 Boundary Conditions

The daily activities as walking and stair-climbing were used in the research. The muscular forces were acted on the proximal femur and the body weight was pressed at the top of femoral head as shown in Fig. 2 under walking and stair-climbing condition [11]. The loading positions were defined by Heller M.O., *et al.* as shown in Table. 4 [12].

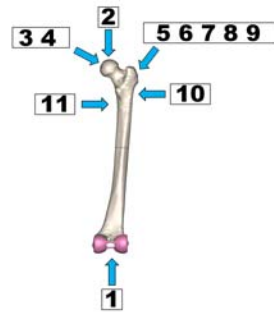


Fig. 2 Boundary condition defined on the proximal femur

Table. 4 The loading on proximal femur under walking and stair-climbing condition [12].

Position	Force	
	Walking	Stair-climbing
1	Fix displacement	Fix displacement
2	Body weight	Body weight
3	Hip contact	Hip contact
4	Intersegmental resultant	Intersegmental resultant
5	Abductor	Abductor
6	-	Ilio-tibial tract, proximal
7	-	Ilio-tibial tract, distal
8	Tensor fascia latae, proximal	Tensor fascia latae, proximal
9	Tensor fascia latae, distal	Tensor fascia latae, distal
10	Vastus lateralis	Vastus lateralis
11	-	Vastus medialis

2.3.1 Dynamic condition

Hip contact and muscular forces were used to analysis under dynamic condition which varied with time. The dynamic walking condition was shown the hip contact and muscular force in Fig. 3 - 7.

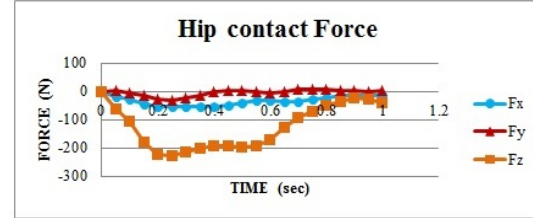


Fig. 3 Hip contact force under dynamic walking condition [13]

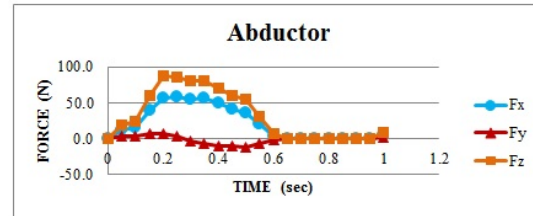


Fig. 4 Abductor force under dynamic walking condition [13]

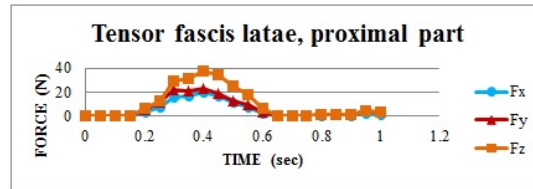


Fig. 5 Tensor fascia latae, proximal part force under dynamic walking condition [13]

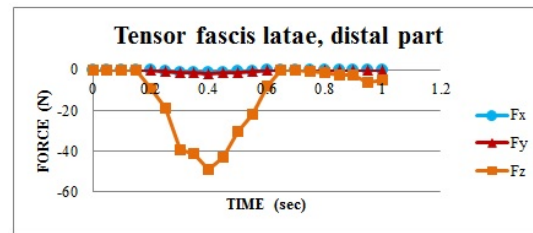


Fig. 6 Tensor fascia latae, distal part force under dynamic walking condition [13]

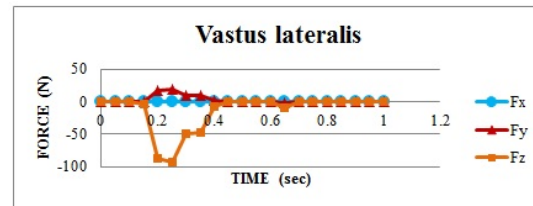


Fig. 7 Vastus lateralis force under dynamic walking condition [13]

POS0009

The dynamic stair-climbing condition was shown the hip contact and the muscular force in Fig. 8 - 15.

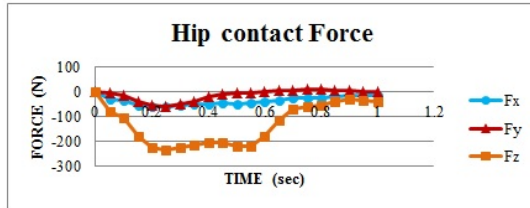


Fig. 8 Hip contact force under dynamic stair-climbing condition [13]

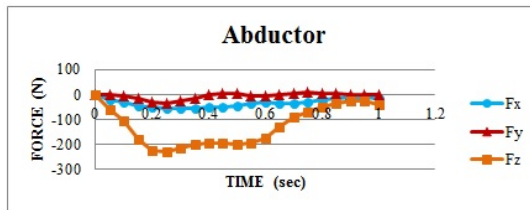


Fig. 9 Abductor force under dynamic stair-climbing condition [13]

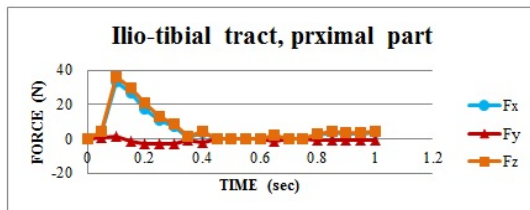


Fig. 10 Ilio-tibial tract, proximal part force under dynamic stair-climbing condition [13]

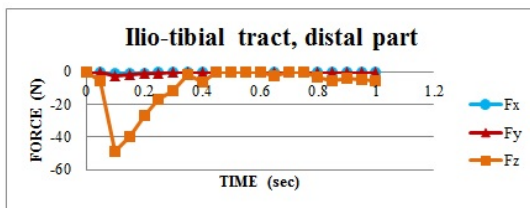


Fig. 11 Ilio-tibial tract, distal part force under dynamic stair-climbing condition [13]

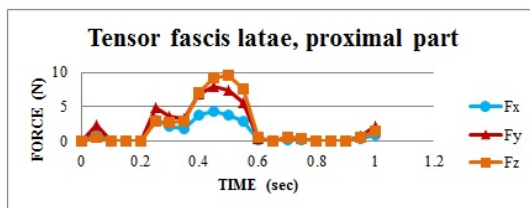


Fig. 12 Tensor fascia latae, proximal part force under dynamic stair-climbing condition [13]

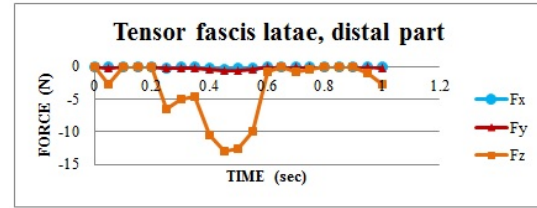


Fig. 13 Tensor fascia latae, distal part force under dynamic stair-climbing condition [13]

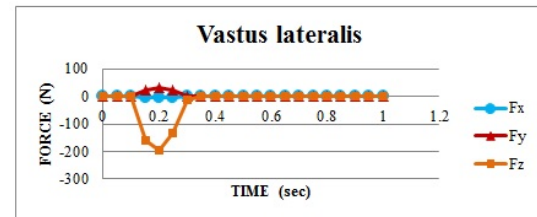


Fig. 14 Vastus lateralis force under dynamic stair-climbing condition [13]

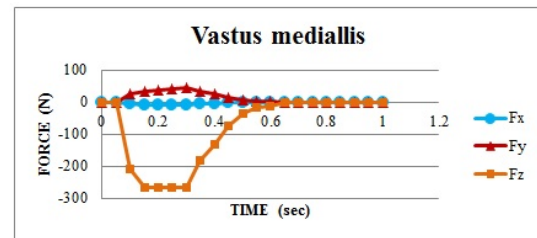


Fig. 15 Vastus medialis force under dynamic stair-climbing condition [13]

All models were drilled pin-track hole at the medial side of femur with a semi-bicortical pattern as shown in Fig. 16, which was varied the hole angle as 10, 15 and 20 degree and the hole diameter as 3 and 4 mm.



Fig. 16 The semi-bicortical of pin-track hole [14]

2.4 Mesh model

Mesh generations were generated by MSC Marc package which include the femoral bone and femoral component. The femur model had a total of 85,123 nodes and 355,893 elements and the femoral component had a total of 6,771 nodes and 26,450 elements. The mesh model of femur-implant was shown in Fig. 17.

POS0009

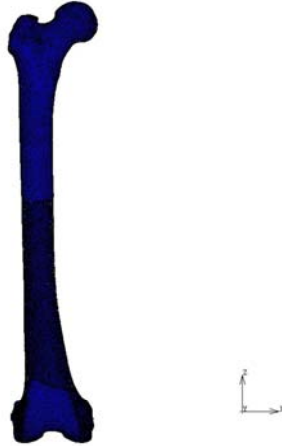


Fig. 17 Mesh model of femur-implant

3. Result and Discussion

This research was evaluated the maximum equivalent of total strain on the femur under dynamic walking and dynamic stair-climbing condition, which were shown in Table. 5 and 6 respectively.

Table. 5 The maximum equivalent of total strain of under dynamic walking condition.

Model	Sex	Age range	Time (Sec)	Size and angle of pin-track hole	Maximum equivalent total strain (microstrain)
Neutral alignment	men	80-89	0.1	4 mm. 15 degree	2,389.59
Neutral alignment	women	60-69	0.1	4 mm. 15 degree	2,753.41
3 degree valgus	men	80-89	0.1	4 mm. 20 degree	1,411.12
3 degree valgus	women	60-69	0.1	4 mm. 20 degree	1,651.77

Table. 6 The maximum equivalent of total strain under dynamic stair-climbing condition.

Model	Sex	Age range	Time (Sec)	Size and angle of pin-track hole	Maximum equivalent total strain (microstrain)
Neutral alignment	men	80-89	0.1	4 mm. 20 degree	2,513.34
Neutral alignment	women	60-69	0.1	4 mm. 20 degree	2,963.35
3 degree valgus	men	80-89	0.1	3 mm. 10 degree	1,244.84
3 degree valgus	women	60-69	0.1	3 mm. 10 degree	1,507.19

3.1 The maximum strain on neutral alignment model

The maximum equivalent of total strain occurred on the neutral alignment model under dynamic condition at the age range 80-89 for men and 60-69 for women. Around the pin-track hole region, the maximum equivalent of total strain distribution for men were 2,389.59 and 2,513.34 microstrain under dynamic walking and dynamic stair-climbing condition as shown in Fig. 17 and for women were 2,753.41 and 2,963.35 microstrain under dynamic walking and dynamic stair-climbing condition as shown in Fig. 18.

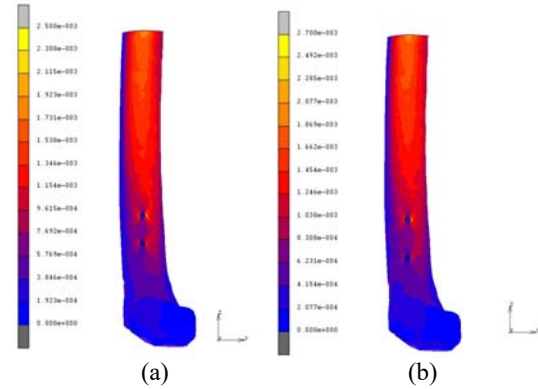


Fig. 17 The maximum equivalent of total strain distribution around pin-track hole region with neutral alignment of men model: (a) dynamic walking and (b) dynamic stair-climbing

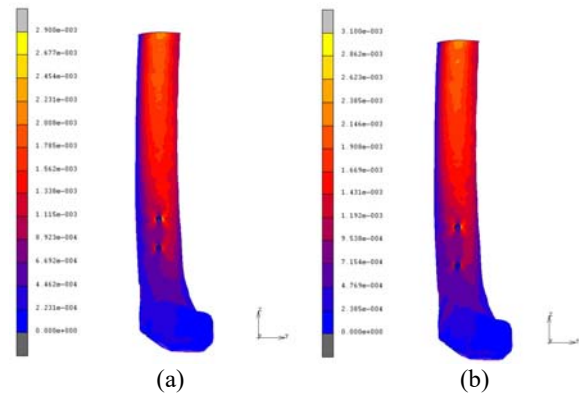


Fig. 18 The maximum equivalent of total strain distribution around pin-track hole region with neutral alignment of women model: (a) dynamic walking and (b) dynamic stair-climbing

3.2 The maximum strain on 3 degree valgus alignment model

The maximum equivalent of total strain occurred on the 3 degree valgus alignment model under dynamic condition at the age range 80-89 for men and 60-69 for women. Around the pin-track hole region, the maximum equivalent of total strain distribution for men were 1,411.12 and 1,244.84 microstrain under dynamic walking and dynamic stair-climbing condition as shown in Fig. 19 and for women were 1,651.77 and 1,507.19 microstrain under dynamic walking and dynamic stair-climbing condition as shown in Fig. 20.

POS0009

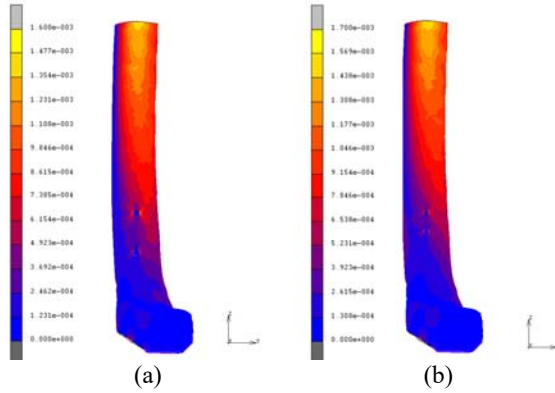


Fig. 19 The maximum equivalent of total strain distribution around pin-track hole region with 3 degree valgus alignment of men model: (a) dynamic walking and (b) dynamic stair-climbing

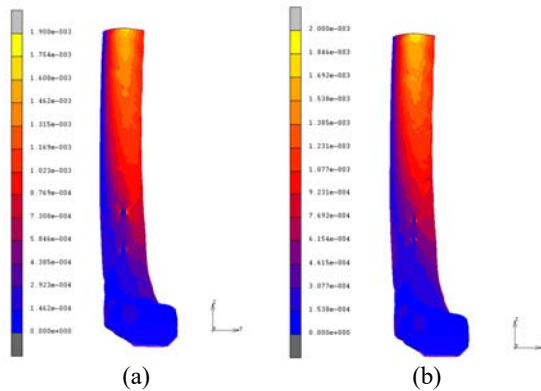


Fig. 20 The maximum equivalent of total strain distribution around pin-track hole region with 3 degree valgus alignment of women model: (a) dynamic walking and (b) dynamic stair-climbing

3.3 Trend of maximum equivalent of total strain to the age of human

The elastic modulus was inverse varied with age in both cases. The decreased elastic modulus made the bone absorbed more energy and the maximum equivalent of total strain had increased. The graph between maximum equivalent of total strain and elastic modulus, was varied with time, on neutral alignment model was shown in Fig. 21.

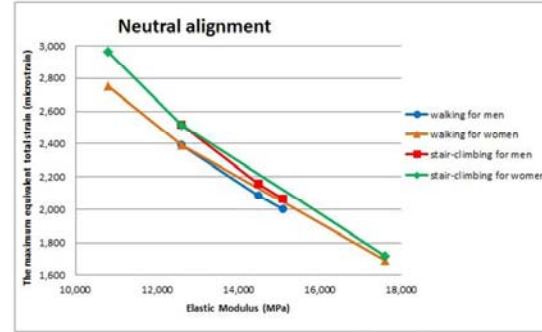


Fig. 21 The maximum equivalent of total strain versus elastic modulus, varied with time of neutral alignment models

The graph between maximum equivalent of total strain and elastic modulus, was varied with time, on 3 degree valgus alignment model was shown in Fig. 22.

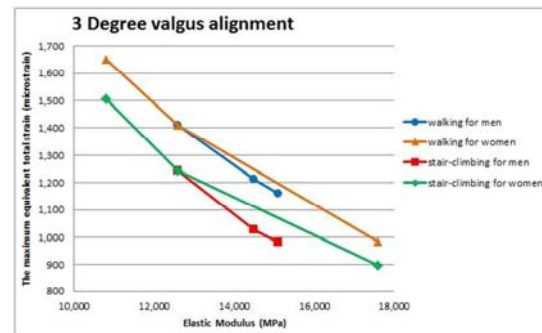


Fig. 22 The maximum equivalent of total strain versus elastic modulus, varied with time of 3 degree valgus alignment models

The elastic modulus of elder model affects the maximum equivalent of total strain distribution around the pin-track hole region under dynamic conditions but the maximum strain did not exceed 25,000 microstrain [15, 16] that the ultimate value of bone fracture. All models of varus bone inserted femoral component did not fracture on pin-track hole under static walking, static stair-climbing, dynamic walking and dynamic stair-climbing condition [2, 3, 17].

4. Conclusion

The total knee replacement surgery should be inserted the femoral component with 3 degree valgus alignment for the lowest maximum equivalent of total strain on the bone [3, 4]. The dynamic loading condition did not affect the femur fracture at the pin-track hole region because the maximum equivalent of total strain on the bone less than 25,000 microstrain. The patient had a femur fracture on post-operatively at the pin-track hole region may be overweight or obese [18] or may be occur under impact or fatigue failure condition.

POS0009

5. Acknowledgement

The authors wish to thank the Faculty of Medicine, Burapha University and Biomechanics Analysis and Orthopedic Device Design Laboratory (B-AODD LAB), Department of Mechanical Engineering, Faculty of Engineering, Mahidol University for their support with facilities.

6. References

- [1] Ewe, T.W., Chee, E.K., Chooi, Y.S. and Ng, W.M. (2010). Causative factors for femoral pin track fractures in navigated total knee arthroplasty. *Malaysian Orthopaedic Journal*, vol. 4(1), pp. 8-11.
- [2] Aungsutanasombat, C., Somtua, C., Aroonjarattham, K. and Aroonjarattham, P. (2015). The comparison of pin-track hole effect on normal and varus femoral bone, paper presented in the 6th International Conference on Mechanical Engineering 2015, Phetchaburi, Thailand.
- [3] Somtua, C., Aroonjarattham, K., Aroonjarattham, P. and Chanasakulniyom, M. (2015). The effect of pin track holes on Thai femur after total knee arthroplasty, paper presented in the 29th Conference of Mechanical Engineering Network of Thailand 2015, Nakhonratchasima, Thailand.
- [4] Aroonjarattham, P., Aroonjarattham, K. and Suvanjumrat, C. (2014). Effect of mechanical axis on strain distribution after total knee replacement. *J. Kasetsart (Nat. Sci.)*, vol. 48(2), pp. 263-282.
- [5] Sitthiseripratip, K., Van Oosterwyck, H., Vander Sloten, J., Mahaisavariya, B., Bohez, E.L.J., Suwanprateeb, J. Van Audekercke, R. and Oris P. (2003). Finite element study of trochanteric gamma nail for trochanteric fracture. *Med Eng&Phy*, vol. 25, pp. 99-106.
- [6] Serala, B., Garc, J.M., Cegon, J., Doblare, M. and Serala, F. (2004). Finite element study of intramedullary osteosynthesis in the treatment of trochanteric fractures of the hip: Gamma and PFN. *J. Care Injured*, vol. 35, pp. 130-135.
- [7] Mahaisavariya, B., Sitthiseripratip, K. and Suwanprateeb, J. (2006). Finite element study of the proximal femur with retained trochanteric gamma nail and after removal of nail. *J. Care Injured*, vol. 37, pp. 778-785.
- [8] Peraz, A., Mahar, A., Negus, C., Newton, P. and Impelluso, T. (2010). A computational evaluation of the effect of intramedullary nail material properties on the stabilization of simulated femoral shaft fracture. *Med Eng & Phys*, vol. 30, pp. 755-760.
- [9] Senapati, S.K. and Pal, S. (2012). Uhnwpe-alumina ceramic composite, an improved prosthesis materials for an artificial cemented hip joint. *Trends biomater: Artif Organs*, vol. 16(1), pp. 5-7.
- [10] Marc, A. and Martens, M.D. (1985). Mechanical properties of human bone, Pellenberg, Belgium.
- [11] El' Sheikn, H.F., MacDnald, B.J. and Hashmi, M.S.J. (2003). Finite element simulation of the hip joint during stumbling a comparison between static and dynamic loading. *Journal of Material Processing Technology*, December 2003, vol. 143-144, pp. 249-255.
- [12] Heller, M.O., Bergmann, G., Kassi, J.P., Cales, L., Haas, N.P. and Duda, G.N. (2005). Deterioration of muscle loading at the hip joint for use in pre-clinical testing. *Journal of Biomechanics*, May 2005, vol. 38, pp. 1155-1163.
- [13] Bregmann, G. (2001). "HIP98", Free University, Berlin.
- [14] Rüber, J., Peyerl, S., Campbell, M. D. and Buehler, K. (2008). Technical aspects of percutaneous pin placement during computer assisted navigated knee arthroplasty in the context of femoral stress fractures. Stryker Leibinger GmbH & Co. KG, Freiburg, Germany.
- [15] Frost, H. M. (1994). Wolff's law and bone's structural adaptation to mechanical usage: an overview for clinicians. *The Angle Orthodontist*, vol. 64(3), pp. 175-188.
- [16] Frost, H. M. (2003). A 2003 Update of Bone Physiology and Wolff's Law for Clinicians. *Angle Orthodontist*, vol. 74, pp. 3-15.
- [17] Sangrit, K., Anuchitchanchai, P., Aroonjarattham, K., Aroonjarattham, P. and Somtua, C. (2016). The effect of pin-track hole on varus femoral bone varied modulus of elasticity, paper presented in the 6th International Conference on Engineering and Applied Sciences 2016, Hong Kong.
- [18] Beldame, J., Boisrenoult, P. and Beaufils, P. (2010). Pin track induced fractures around computer-assisted TKA. *Orthopaedics & Traumatology: Surgery & Research*, vol. 96, pp. 249-255.